Biosensors and Bioelectronics 31 (2012) 357–362

Contents lists available at SciVerse ScienceDirect

Biosensors and Bioelectronics

journal homepage: www.elsevier.com/locate/bios

Fabrication of a chitosan/glucose oxidase–poly(anilineboronic acid)–Au_{nano}/Au-plated Au electrode for biosensor and biofuel cell

Yi Huang [a], Xiaoli Qin [a], Zou Li [a], Yingchun Fu [a], Cong Qin [a], Feng Wu [a], Zhaohong Su [a], Ming Ma [a], Qingji Xie [a,*], Shouzhuo Yao [a,*], Jiming Hu [b]

[a] Key Laboratory of Chemical Biology and Traditional Chinese Medicine Research (Ministry of Education of China), College of Chemistry and Chemical Engineering, Hunan Normal University, Changsha 410081, China
[b] Key Laboratory of Analytical Chemistry for Biology and Medicine (Ministry of Education of China), Wuhan University, Wuhan 430072, China

ARTICLE INFO

Article history:
Received 29 July 2011
Received in revised form 22 October 2011
Accepted 24 October 2011
Available online 31 October 2011

Keywords:
Poly(anilineboronic acid)
Gold nanoparticles
Glucose oxidase
Glucose biosensing
Biofuel cell

ABSTRACT

Enzyme immobilization is one of the key factors in constructing high-performance enzyme biosensors and biofuel cells (BFCs). Herein, we propose a new protocol for efficient immobilization of a glycoprotein enzyme based on the interaction of the 1, 2- or 1, 3-diols in the glycoprotein with a boronic acid functionalized monomer. Briefly, casting a mixture of glucose oxidase (GOx) and anilineboronic acid (ABA) followed by a $NaAuCl_4$ solution to an Au-plated Au electrode surface yielded a GOx–poly(ABA) (PABA)–gold nanoparticle (Au_{nano}) bionanocomposite, and chitosan (CS) was then cast and air-dried. In the present protocol, the small-sized Au_{nano} or Au subnanostructures can form near/on the enzyme molecule, which greatly promotes the electron transfer of enzymatic reaction and enhances the amperometric responses. The thus-prepared CS/GOx–PABA–Au_{nano}/Au-plated Au electrode worked well in the first-/second generation biosensing modes and as a bioanode in a monopolar biofuel cell, with analytical or cell-power performance superior to those of most analogues hitherto reported.

1. Introduction

Immobilization of biomacromolecules at high load/bioactivity is the crucial step to construct various electrochemical biosensors, and the immobilization matrix and strategy can largely affect their biosensing performance (Mateo et al., 2007). Many biocompatible polymer matrices, which adheres strongly to the electrode surface and provides a suitable environment for biomacromolecules, are excellent candidates for biomacromolecular immobilization (Rahman et al., 2005). Electrically conducting nanomaterials, which can promote electron transfer of the target with the electrode, have been widely used to fabricate amperometric biosensors at improved electroanalytical performance (Sanchez et al., 2011; Sarma et al., 2009).

Boronic acid functionalized compounds have attracted much attention in both chemistry and biology. Boronic acid can reversibly form chemical bonds with 1, 2- or 1, 3-diols to generate five or six-membered cyclic complexes (Springsteen and Wang, 2002). Hence, the boronic acid structure is widely used as the recognition motif for chemo/biosensing (Fang et al., 2004; Frasconi et al., 2010; Mader and Wolfbeis, 2008; Matsumoto et al., 2009; Shoji and Freund, 2001; Zhong et al., 2010) and enrichment and separation of biomolecules (Liang and Liu, 2011; Lin et al., 2011; Xu et al., 2009; Yao et al., 2008; Yeap et al., 2008). Boronic acid functionalized compounds have also been used to assemble supermolecules and nanocomposites (Burress et al., 2010; Fujita et al., 2008) and immobilize diols-containing molecules (Hsiao et al., 2010; Pham et al., 2010). Many proteins can be glycosylated in vivo and in vitro to form glycoproteins, including many enzymes and antibodies, and the immobilization of glycoproteins based on boronic acid–diols interaction has thus attracted much attention. The feasibility of using carbohydrates as binding motifs makes it an interesting alternative to other covalent immobilization procedures that compromise amino acid residues. The Willner's group realized the electrical wiring of redox enzyme by the bridging action between boronic acid and FAD or $NAD(P)^+$ cofactor through boronate ester bond formation, and then *apo*-GOx or dehydrogenase was bound to yield an electrically wiring enzyme monolayer. The resulting reconstituted enzyme reveals effective electrical contact with the electrode for enhanced amperometric analysis (Yan et al., 2007; Zayats et al., 2002a,b). Another enzyme, horseradish peroxidase, was also immobilized on phenylboronic acid self-assembled monolayers (Abad et al., 2002; Liu et al., 2005). Glycoprotein antibody was also immobilized on boronic acid self-assembly layer in an oriented manner, and most of the epitopes of the bound antibodies were

* Corresponding author. Tel.: +86 731 88865515; fax: +86 731 88865515.
E-mail address: xieqj@hunnu.edu.cn (Q. Xie).

0956-5663/$ – see front matter © 2011 Elsevier B.V. All rights reserved.
doi:10.1016/j.bios.2011.10.045

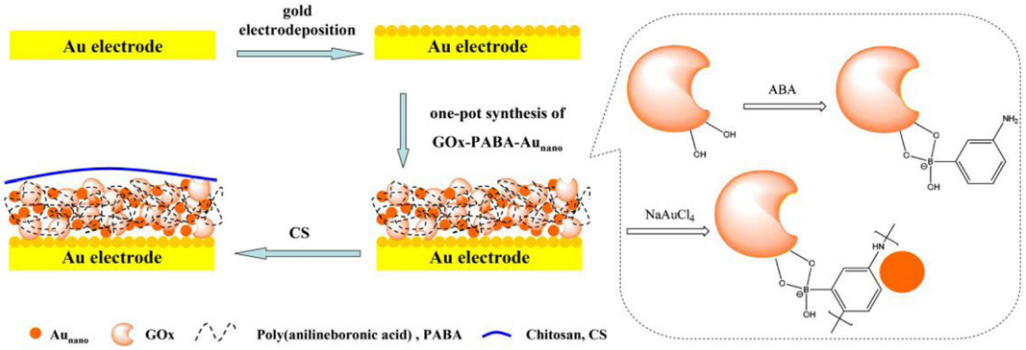

Scheme 1. Procedures and principle for preparing the CS/GOx–PABA–Au_{nano}/Au-plated Au enzyme electrode.

directed towards the solution, leading to a significant improvement in sensitivity for immunoanalysis (Ho et al., 2010; Lin et al., 2009; Zhang et al., 2008). As far as we know, the entrapment of glycosylated molecules into boronic acid based polymer matrix for biosensors and biofuel cells (BFC) was not reported.

Herein, a novel, simple and rather universal approach for immobilization of glycoproteins is reported. Glucose oxidase (GOx), a flavoenzyme that is glycosylated to 16–25 wt.%, was chosen as a model glycoprotein enzyme. As shown in Scheme 1, on an Au-plated Au electrode, anilineboronic acid (ABA) as a functional reagent is linked to the sugar groups of GOx, and its aniline moiety and excess solution-state ABA can react with $NaAuCl_4$ to yield the bionanocomposite of Au nanoparticles (Au_{nano}), poly(anilineboronic acid) (PABA), and GOx in an one-pot manner. An outer-layer chitosan film was then coated on the electrode surface. The thus-prepared enzyme electrode possesses good biosensing performance, which is also demonstrated as an excellent bioanode in BFC construction.

2. Experimental

2.1. Instrumentation and chemicals

All electrochemical experiments were conducted on a CHI660C electrochemical workstation (CH Instrument Co.), and a conventional three-electrode electrolytic cell was used. The gold disk electrode with 2 mm diameter served as the working electrode. The reference electrode was a KCl-saturated calomel electrode (SCE), and a carbon rod served as the counter electrode. All potentials reported here are cited versus the SCE. A computer-interfaced HP4395A impedance analyzer was employed in the quartz crystal microbalance (QCM) experiments, and AT-cut 9 MHz gold-coated piezoelectric quartz crystals (PQCs, 1.25-cm diameter, Model JA5, Beijing Chenjing Electronics Co., Ltd., China) were used (Fu et al., 2008). Transmission electron microscopy (TEM) images were collected on a Hitachi 800 transmission electron microscope. UV–vis spectra were recorded on a UV2450 spectrophotometer (Shimadzu Co., Kyoto, Japan).

GOx (EC 1.1.3.4; type II from *Aspergillus niger*, activity $\approx 150\,kU\,g^{-1}$, MW ≈ 154 kDa), 3-aminophenylboronic acid monohydrate, and dopamine were purchased from Sigma. Chloroauric acid ($HAuCl_4$) and trisodium citrate were purchased from Shanghai Chemicals Station (Shanghai, China). Aniline and pyrrole were purchased from Shantou Xilong Chemical Engineering Factory (Guangdong, China) and Sinopharm Chemical Reagent Co., Ltd. (Shanghai, China), respectively, which were purified via double distillation and stored in a refrigerator prior to use. Chitosan (CS) from crab shells (90% deacetylated) and *p*-benzoquinone (BQ) were also purchased from Sinopharm Chemicals Co., Ltd. (Shanghai, China). Ferrocene monocarboxylic acid (FcMA) was purchased from Suzhou Time-Chem Technologies Co., Ltd. (Suzhou, China). Nafion (5 wt.%, in a mixture of water and lower aliphatic alcohols) was purchased from Aldrich (USA). All other chemicals were of analytical grade or better quality and used as received. 0.10 M pH 7.0 phosphate buffer solution (PBS) was used. 0.50 wt.% CS solution was prepared in 0.10 M acetate buffer solution (pH 5.4). Glucose stock solution was allowed to mutarotate overnight at room temperature before use. The human serum samples were obtained from Hunan Normal University Hospital. Milli-Q ultrapure water (Millipore, $\geq 18\,M\Omega\,cm$) was used throughout. All experiments were performed at room temperature around 25 °C.

2.2. Procedures

The bare Au electrode was cleaned according to the reported protocol (Zhang et al., 2007). Briefly, the Au electrode was carefully polished in 0.5 and 0.05 μm alumina suspensions in sequence. After being thoroughly rinsed with water, the polished electrode was ultrasonically treated sequentially in water, ethanol, and water for 5 min each to remove residual alumina powder. Then, the Au electrode was treated with Piranha solution (H_2SO_4:H_2O_2, 3:1 in v/v) for 15 s. Afterwards, the Au electrode was subjected to electrochemical rinsing in 0.50 M H_2SO_4 to remove impurities, namely, potentiostatic treatments at 2 V for 5 s and at −0.35 V for 10 s and potential cycling for 6 cycles from −0.35 to 1.55 V at a scan rate of $4\,V\,s^{-1}$. The cleaned Au electrode was finally characterized by cyclic voltammetry from −0.35 to 1.55 V in 0.50 M H_2SO_4, which showed a single sharp reduction peak at ca. 0.9 V and multiple overlapping oxidation peaks at potentials ranging from 1.2 to 1.5 V.

The preparation of enzyme electrode is shown in Scheme 1 and explained in detail as follows.

Firstly, gold was electroplated on the cleaned Au electrode by multi potential step electrolysis from 1.1 to 0 V with a pulse width of 0.25 s in 0.50 M aqueous H_2SO_4 containing 2.0 mM $HAuCl_4$, and the total time for the electrodeposition experiment was 300 s (Tang et al., 2008). The roughness factor (R_f) of the Au-plated Au electrode, which is defined as the ratio of the real electrode-surface area to the geometric area, was determined by the oxygen-adsorption method reported previously (Douglass Jr et al., 2008; Trasatti and Petrii, 1991). Briefly, the Au electrode before and after Au electrodeposition was subjected to cyclic voltammetric experiments (−0.1 to 1.2 V, $50\,mV\,s^{-1}$) in 0.1 M PBS, and the electric charge under the reduction peak of Au oxides was recorded to estimate the R_f.

Secondly, the GOx–ABA composite was prepared by dissolving 10 mg GOx and 5 mg ABA in 1 mL PBS and shaking the solution for 30 min to achieve reaction equilibrium. Then, 2.5 μL GOx–ABA mixture and then 1 μL of 19.7 mM $NaAuCl_4$ were cast on the Au-plated Au electrode for 40-min reaction.

Finally, 1.5 μL of 0.50 wt.% CS solution was cast-dried to prevent enzyme leaching and mechanically strengthen the enzyme film

(CS/GOx–PABA–Au_{nano}/Au-plated Au), and CS as a polysaccharide biopolymer was selected here due to its excellent film-forming ability, biocompatibility, high water permeability, high mechanical strength and good adhesion (Wu et al., 2007; Zhou et al., 2007). The enzyme electrode was rinsed with water several times and potentiostatically treated at 0.70 V for 300 s to electropolymerize residual ABA monomers before use. For comparison, aniline, pyrrole and dopamine were used instead of ABA to prepare GOx-based electrodes following the same procedures as above, which are denoted as CS/GOx–polyaniline (PANI)–Au_{nano}/Au-plated Au, CS/GOx–polypyrrole (PPY)–Au_{nano}/Au-plated Au, CS/GOx–polydopamine (PDA)–Au_{nano}/Au-plated Au, respectively. In addition, gold nanoparticles (AuNPs) were prepared according to the citrate reduction method (Grabar et al., 1995), and the GOx–AuNPs mixture was cast to form CS/GOx–AuNPs/Au-plated Au electrode. When not in use, the prepared enzyme electrodes were stored in PBS at 4 °C (refrigerator).

In the first-generation biosensing mode, the enzyme electrodes were tested by potentiostating them at 0.70 V under solution-stirred conditions to detect oxidation of enzymatically generated H_2O_2. The response current was marked with a change in value between the steady state current after substrate addition and the initial background current without substrate. In the second-generation biosensing mode, cyclic voltammetry in quiescent solution was used for the mediator FcMA, and chronoamperometry at 0.40 V in stirred solution was used for the mediator BQ.

A monopolar glucose BFC was constructed with a CS/GOx–PABA–Au_{nano}/Au-plated Au electrode as the bioanode in 20 mL PBS containing 4.0 mM BQ and 60 mM glucose and a carbon rod as the cathode in Nafion-membrane-isolated 0.40 M $KMnO_4$ + 0.60 M H_2SO_4 aqueous solution, and the cell voltage (U_{cell}) and current (i_{cell}) of the BFC at varying external resistance loads (R_e) were dynamically monitored with the electrochemical noise module of an Autolab PGSTAT30 electrochemical workstation (The Netherlands) (Chen et al., 2011; Tan et al., 2008, 2009).

The QCM technique was used to evaluate the boronic acid–diols interaction between PABA in enzyme film and glucose in solution. The enzyme film modified PQC Au electrode were prepared by successively casting 10 μL GOx–ABA composite containing 0.2 mg mL^{-1} GOx and 0.1 mg mL^{-1} ABA, 2 μL 0.8 mM $NaAuCl_4$ and 5 μL 0.05 wt.% CS on a PQC Au electrode to form a CS/GOx–PABA–Au_{nano}/PQC Au electrode after solvent evaporation. For comparison, 5 μL 0.05 wt.% Nafion (obtained by dilution with absolute ethanol) was used instead of CS to prepare a Nafion/GOx–PABA–Au_{nano}/PQC Au electrode. Furthermore, a PABA film was electrodeposited by cyclic voltammetry (−0.2 to 0.8 V, 50 mV s^{-1}), as shown in Fig. S1 in the Supplementary Data, and the thickness of PABA film was controlled to $\Delta f_0 = -400 \pm 10$ Hz.

3. Results and discussion

3.1. Fabrication and characterization of enzyme electrodes

An electrode with improved surface roughness can usually be used for biosensing with improved sensitivity (Qiu et al., 2009; Seker et al., 2009). Here, we used a multi potential step technique to increase the surface roughness of the Au electrode, in order to enhance the biosensing sensitivity. As shown in Fig. S2 in the Supplementary Data, cyclic voltammetry experiments for bare Au and Au-plated Au electrodes were performed in 0.1 M PBS. The R_f was determined by the oxygen-adsorption experiment at each Au electrode (Douglass Jr et al., 2008; Hoogvliet et al., 2000). The ratio of the reduction charge of gold oxides to the standard value for monolayer oxygen adsorption, 390 μC cm^{-2}, is the real electrode-surface area (Douglass Jr et al., 2008; Trasatti and Petrii, 1991). The R_f value is the ratio of the real electrode-surface area to the geometric area. The charges under the gold oxide reduction peak increased from 21.9 to 59.4 μC after gold electrodeposition, and the R_f values of bare Au and Au-plated Au electrode (geometric area = 0.031 cm^2) are calculated to be 1.8 and 4.9, respectively. As expected, the roughened Au-plated Au electrode shows better electrocatalytic activity than the bare Au electrode towards H_2O_2 oxidation (Fig. S3 in the Supplementary Data). The quantity of the plated Au was optimized (300-s plating) according to the electrocatalytic activity towards H_2O_2 oxidation, as given in Fig. S4 in the Supplementary Data.

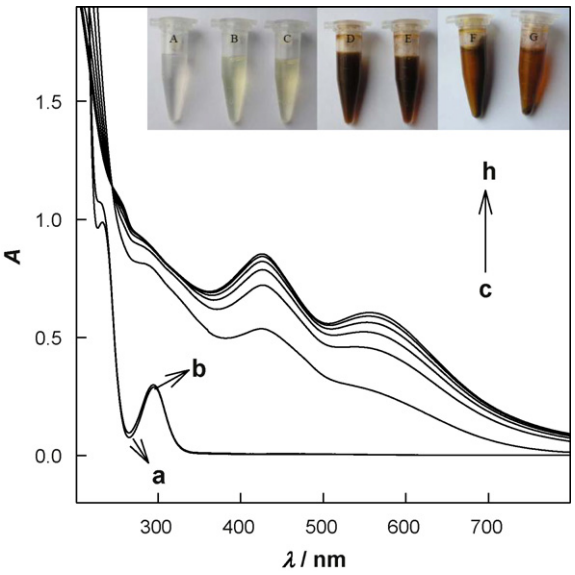

Fig. 1. UV–vis absorption spectra of 0.02 mg mL^{-1} ABA aqueous solution (a), 0.02 mg mL^{-1} ABA + 0.04 mg mL^{-1} GOx aqueous solution (b), and 0.02 mg mL^{-1} ABA + 0.04 mg mL^{-1} GOx + 2 μM $NaAuCl_4$ (c–h, recorded every 1 min). Insert: photographs of ABA (A), GOx (B) and GOx–ABA (C) aqueous solutions, followed by addition of $NaAuCl_4$ into A and C and subsequent quiescence for 3 min (D and E, respectively), and centrifugation for 10 min at 10,000 rpm (F and G, respectively).

$NaAuCl_4$ is used here as a chemical oxidant to polymerize ABA in aqueous solution in the presence of GOx, and many conducting Au nanoparticles can be produced simultaneously. UV–vis spectroscopy was employed to monitor the formation of the bionanocomposite. As shown in Fig. 1, ABA gave an absorption peak at 294 nm, and two new absorption bands peaking at about 420 and 555 nm could be observed after $NaAuCl_4$ addition. The absorption band at 420 nm is assigned to polaron absorption band related to the doping level of polyaniline backbone (Khiew et al., 2004), and the absorption band at 555 nm may result from the plasmon adsorption of gold nanoparticles. The insert of Fig. 1 shows the visual inspection results. As soon as $NaAuCl_4$ was added into the transparent and colorless ABA aqueous solution, the solution turned to be turbid and red brown in color, indicating the immediate onset of ABA oxidation/polymerization and Au_{nano} formation to form two-component PABA–Au_{nano} nanocomposite. Similar phenomena were observed after adding $NaAuCl_4$ to the GOx–ABA solution, but more precipitates were collected after 10-min centrifugation in the presence of GOx, implying the formation of three-component GOx–PABA–Au_{nano} bionanocomposite. The TEM image of the GOx–PABA–Au_{nano} bionanocomposite is shown in Fig. S5 in the Supplementary Data, which shows that the bionanocomposite contains much Au nanoparticles of a statistically dominant size of 19 nm. Au nanoparticles of ~19 nm size should commonly have a plasmon absorption peak at ~520 nm (Link and El-Sayed, 1999), but we observed the Au_{nano} peaks at ca. 555 nm, indicating the polymer shell in the bionanocomposite can affect the plasmon absorption of Au_{nano}, and similar strong red-shift

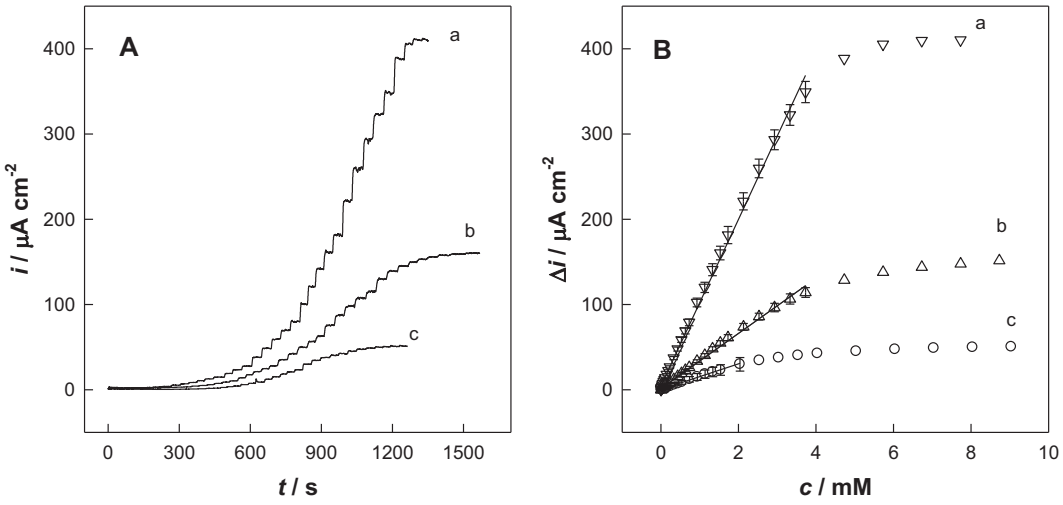

Fig. 2. Chronoamperometric responses (A) to successive additions of glucose and the calibration curves (B) on CS/GOx–PABA–Au_{nano}/Au-plated Au (a), CS/GOx–PANI–Au_{nano}/Au-plated Au (b), and CS/GOx–AuNPs/Au-plated Au (c) electrodes at 0.7 V in pH 7.0 PBS, respectively. The enzyme electrodes were fabricated under optimized conditions. The linearly regressed lines are also shown.

phenomena were also reported in literatures (Ma et al., 2005; Tokareva et al., 2004; Zhou et al., 2002).

3.2. Biosensing performance in the first-generation biosensing mode

To obtain the best sensitivity for glucose assay, various conditions for preparation of the enzyme film were optimized according to the first-generation biosensing output via variation of the examined one while others fixed, as listed in Table S1 in the Supplementary Data. Here, ABA (32.3 mM) is in excess versus the glycated quantity of GOx (equivalent to 8.9–13.9 mM glucose unit, as estimated at a glycosylated percentage of GOx of 16–25 wt.% (Courjean et al., 2009)), and the excess ABA can sufficiently reduce $NaAuCl_4$ to produce more Au_{nano} for increased biosensing sensitivity. The cast volume of 0.50 wt.% CS was optimized as 1.5 μL.

To test the performance of the biosensors, the steady-state currents for several enzyme electrodes under optimized conditions were examined in stirred PBS in the first-generation biosensing mode. The amperometric glucose-biosensing responses (panel A) and the calibration curves (panel B) of several enzyme electrodes are shown in Fig. 2 and Fig. S6 in the Supplementary Data, and the values of sensitivity, limit of detection (LOD, $S/N = 3$), and linear detection range (LDR) are listed in Table 1. The amperometric response at CS/GOx–PABA–Au_{nano}/Au-plated Au electrode was linear with glucose concentration from 2 μM to 3.7 mM with a sensitivity of 97.7 $\mu A\,mM^{-1}\,cm^{-2}$. The sensitivity is the best as compared with the cases of using other monomers and the monomer-free case. The sensitivity in the PDA case ranks the second, since PDA is also proven a nice matrix for biomacromolecular immobilization (Fu et al., 2009; Tan et al., 2010). Our CS/GOx–PABA–Au_{nano}/Au-plated Au biosensor shows the highest sensitivity and the lowest LOD, as compared with the controls and the reported results (Table 1). The reasons may be as follows. The boronic acid group-containing ABA monomer can tether the glycoprotein enzyme, and the small-sized Au_{nano} or subnanostructures of Au can thus be produced near/on the enzyme molecule after $NaAuCl_4$ addition, as schematically shown in Fig. S7 in the Supplementary Data, which greatly promotes the electron transfer of enzymatic reaction and enhances the amperometric sensitivity.

The apparent Michaelis–Menten constant (K_m^{app}), which can be calculated from the Lineweaver–Burk equation (Dixon, 1953), is an indicator of the enzyme–substrate kinetics. From the slope and intercept of the Lineweaver–Burk plot, we obtain the value of K_m^{app} for the CS/GOx–PABA–Au_{nano}/Au-plated Au electrode as 2.8 mM, which is lower than the reported values of 4.3 mM for

Table 1
Performance of some typical glucose biosensors based on Au_{nano}-relevant matrices.

Fabrication	Sensitivity/μA mM^{-1} cm^{-2}	LOD/μM	LDR/mM	References
AuNP–GOx–Nafion/GCE	0.4	370	1–20	Thibault et al. (2008)
CS–GOx–AuNP/Au		2.7	0.005–2.4	Luo et al. (2004)
Nafion/GOx–AuNP/GCE	6.5	34		Zhao et al. (2006)
Gox/MAA/AuNPs/TiO_2NT/Ti		310	0.4–8	Zhang et al. (2011)
GOx/AuNP/CS/GOx/AuNP/PAA/Pt		7.0	0.5–16	Wu et al. (2007)
Nafion/GOx/Au–MWNT/GCE	5.71	20	0.05–22	Rakhi et al. (2009)
$(GOx–AuNP)_n$/Au	5.72	8.0	0.01–13	Yang et al. (2006)
GOx–CS–AuNP/PB/GCE	69.3	0.69	0.001–1.6	Xue et al. (2006)
Nafion/GOx/AuNP/PANI/PS/GCE		12	0.04–2.0	Liu et al. (2008)
CS/GOx/Au-plated Au	12.1			This work
CS/GOx–PABA/Au-plated Au	7.2			This work
CS/GOx–PABA–Au_{nano}/Au	72.1	0.5	0.004–2.9	This work
CS/GOx–AuNPs/Au-plated Au	15.0	2.0	0.01–2.0	This work
CS/GOx–PPY–Au_{nano}/Au-plated Au	31.8	1.0	0.005–1.8	This work
CS/GOx–PDA–Au_{nano}/Au-plated Au	73.6	0.5	0.005–2.4	This work
CS/GOx–PANI–Au_{nano}/Au-plated Au	33.3	1.2	0.005–3.7	This work
CS/GOx–PABA–Au_{nano}/Au-plated Au	97.7	0.1	0.002–3.7	This work

GCE: glassy carbon electrode; PS: polystyrene; PB: prussian blue; MAA: mercaptoacetic acid; PAA: poly(allylamine); and MWNT: multiwalled carbon nanotube.

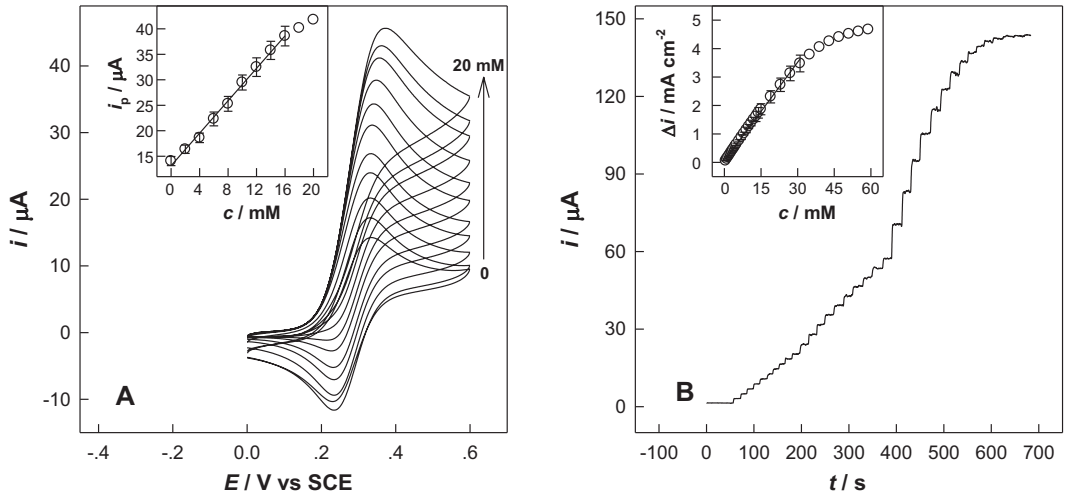

Fig. 3. (A) Cyclic voltammogram and the calibration curve of the anodic peak current (insert) of a CS/GOx–PABA–Au_{nano}/Au-plated Au electrode in degassed PBS containing 4 mM FcMA and 0, 2, 4, 6, 8, 10, 12, 14, 16, 18, or 20 mM glucose. Scan rate: 50 mV s^{-1}. (B) Chronoamperometric responses to successive additions of glucose and the calibration curve (insert) of a CS/GOx–PABA–Au_{nano}/Au-plated Au electrode at 0.4 V in degassed PBS containing 4 mM BQ.

GOx immobilized on AuNPs monolayer modified Au electrode (Zhang et al., 2005) and 7.2 mM for GOx immobilized at AuNPs modified TiO_2 nanotube array electrode (Zhang et al., 2011). Such a small K_m^{app} value may be attributed to the fact that the PABA–Au_{nano} nanocomposite can immobilize the enzyme at high load/activity. The anti-interference ability against ascorbic acid (AA) and uric acid (UA) was also examined. As shown in Fig. S8 in the Supplementary Data, the additions of 0.1 mM AA and UA caused negligible interference to the detection of glucose. The potential of practical usage of the biosensor was validated with several human serum samples and the values measured at CS/GOx–PABA–Au_{nano}/Au-plated Au electrode agreed well with the hospital results (Table S2 in the Supplementary Data).

The reproducibility and storage stability of the biosensor were investigated by amperometric measurements. The reproducibility of this biosensor is evaluated with relative standard deviation of 4.2% ($n = 5$) for 1 mM of glucose. In addition, the long-term stability is also tested by measuring the glucose concentration in a month, as shown in Fig. S9 in the Supplementary Data. It is revealed that the current response of the sensor maintains 85% of the initial current response after 1 month.

The boronic acid–diols interaction between PABA in the enzyme film and glucose in solution was evaluated by the QCM technique, as shown in Fig. S10 in the Supplementary Data. When 1 mM glucose was added into stirred 0.1 M PBS (pH 7.0), the frequency decreased by 70 Hz at PABA/PQC Au electrode and by 45 Hz at Nafion/GOx–PABA–Au_{nano}/PQC Au electrode, while a negligible frequency response was observed on CS/GOx–PABA–Au_{nano}/PQC Au electrode, indicating that polysaccharide CS could efficiently block the residual boronic acid binding sites.

3.3. Biosensing performance in the second-generation biosensing mode and BFC construction

The dissolved O_2 acts as a natural mediator for GOx turnover, but it is of only about 1.3 mM saturated concentration in water, thus the deficiency of O_2 limits the LDR and the saturated current of the first-generation oxidase-based biosensor (Wang, 2008). Here, the proposed enzyme biosensors were also examined for the possibility to develop the second-generation biosensing mode using conventional redox mediators of FcMA and BQ. As shown in Fig. 3A, FcMA exhibited well-defined redox peaks

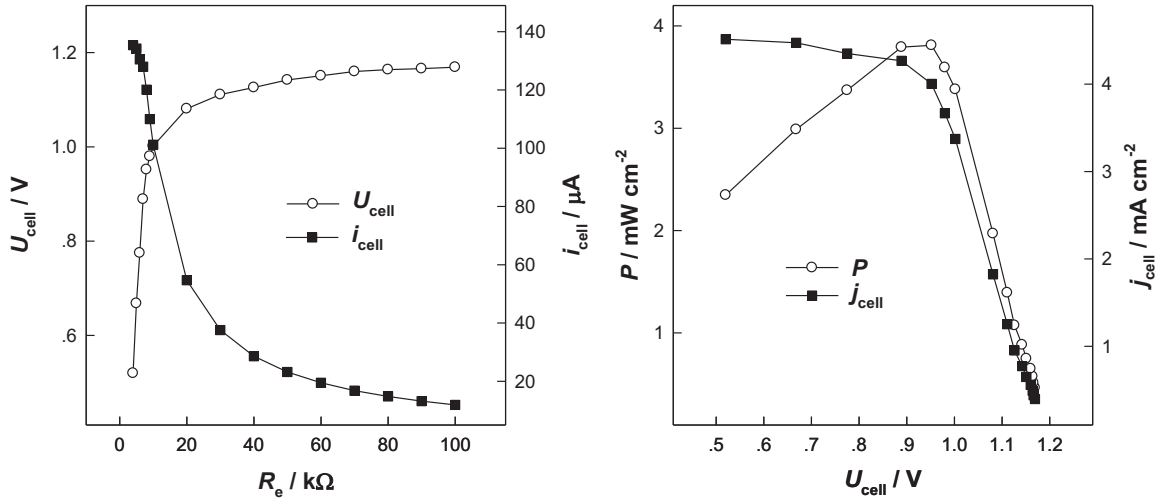

Fig. 4. i_{cell} and U_{cell} as functions of R_e as well as j_{cell} and P as functions of U_{cell} for the monopolar BFC fabricated as detailed in the text.

centering at ca. 0.3 V on CS/GOx–PABA–Au_{nano}/Au-plated Au electrode, and successive additions of glucose increased the anodic peak and decreased the cathodic peak, and the anodic peak current is linear with the glucose concentration (insert), highlighting the mediator effect of FcMA on GOx. In the presence of 4 mM FcMA, the LDR was favorably extended to 16 mM with a slope of 1.6 $\mu A\,mM^{-1}\,cm^{-2}$. The current responses and the calibration curves of the CS/GOx–PABA–Au_{nano}/Au-plated Au electrode to glucose in the presence of 4 mM BQ at a detection potential of 0.4 V are shown in Fig. 3B. The LDR was favorably extended to 31 mM with a sensitivity as high as 115 $\mu A\,mM^{-1}\,cm^{-2}$, and the glucose-saturated current density can reach ca. 5.0 $mA\,cm^{-2}$. The above results demonstrate that the prepared enzyme electrode can evolve into second-generation biosensors by simple addition of a redox mediator in the detection solution.

A monopolar BFC based on the prepared enzyme film was fabricated as detailed in Section 2. As shown in Fig. 4, it exhibited an open-circuit potential of 1.23 V, a short-circuit current of 4.47 $mA\,cm^{-2}$, and a maximum power density (P_{max}) of 3.81 $mW\,cm^{-2}$. This P_{max} is much larger than most reported values, indicating the enzyme film here is an excellent anodic material for BFC development (Chen et al., 2011; Kwon et al., 2010; Lee et al., 2010; Nien et al., 2010; Shim et al., 2011; Yu et al., 2010).

4. Conclusions

In summary, we have described a novel one-pot approach to prepare new GOx–PABA–Au_{nano} bionanocomposite for constructing high-performance amperometric biosensor and BFC. The appropriate combination of the boronic acid–diols reaction and Au_{nano} formation can immobilize the glycoprotein enzyme highly efficiently and make the small-sized Au (sub) nanostructures formed near/on the GOx for enhanced electron transfer. The thus-prepared enzyme electrode worked well for biosensing with high sensitivity (97.7 $\mu A\,mM^{-1}\,cm^{-2}$ in the first-generation biosensing mode and 115 $\mu A\,mM^{-1}\,cm^{-2}$ in the second-generation biosensing mode) and for BFC construction (3.81 $mW\,cm^{-2}$). The proposed protocol to synthesize the glycoprotein–polymer–nanomaterial bionanocomposite is simple, convenient and fast in operation, which is expected to find wide biosensing and bioelectronic applications.

Acknowledgments

This work was supported by the National Natural Science Foundation of China (21175042, 21075036, 20875029, 21105026), the State Special Scientific Project on Water Treatment (2009ZX07212-001-06), the Foundations of Hunan Provincial Education Department, Program for Science and Technology Innovative Research Team in Higher Educational Institutions of Hunan Province, State Key Laboratories of Chemo/Biosensing and Chemometrics (200902) and Key Laboratory of Analytical Chemistry for Biology and Medicine (Wuhan University), Ministry of Education.

Appendix A. Supplementary data

Supplementary data associated with this article can be found, in the online version, at doi:10.1016/j.bios.2011.10.045.

References

Abad, J.M., et al., 2002. J. Am. Chem. Soc. 124, 12845–12853.
Burress, J.W., et al., 2010. Angew. Chem. Int. Ed. 49, 8902–8904.
Chen, C., et al., 2011. Biosens. Bioelectron. 26, 2311–2316.
Courjean, O., Gao, F., Mano, N., 2009. Angew. Chem. Int. Ed. 48, 5897–5899.
Dixon, M., 1953. Biochem. J. 55, 170–171.
Douglass Jr., E.F., et al., 2008. Anal. Chem. 80, 7670–7677.
Fang, H., Kaur, G., Wang, B., 2004. J. Fluoresc. 14, 481–489.
Frasconi, M., Tel-Vered, R., Riskin, M., Willner, I., 2010. Anal. Chem. 82, 2512–2519.
Fu, Y., et al., 2008. Anal. Chem. 80, 5829–5838.
Fu, Y., et al., 2009. Adv. Funct. Mater. 19, 1784–1791.
Fujita, N., Shinkai, S., James, T.D., 2008. Chem. Asian J. 3, 1076–1091.
Grabar, K.C., Freeman, R.G., Hommer, M.B., Natan, M.J., 1995. Anal. Chem. 67, 735–743.
Ho, J.A., et al., 2010. Biosens. Bioelectron. 26, 1021–1027.
Hoogvliet, J., Dijksma, M., Kamp, B., Van Bennekom, W., 2000. Anal. Chem. 72, 2016–2021.
Hsiao, H.Y., et al., 2010. Chem. Commun. 47, 1187–1189.
Khiew, P., Huang, N., Radiman, S., Ahmad, M., 2004. Mater. Lett. 58, 516–521.
Kwon, K.Y., et al., 2010. Biosens. Bioelectron. 26, 655–660.
Lee, J.Y., Shin, H.Y., Kang, S.W., Park, C., Kim, S.W., 2010. Biosens. Bioelectron. 26, 2685–2688.
Liang, L., Liu, Z., 2011. Chem. Commun. 47, 2255–2257.
Lin, P., et al., 2009. Anal. Chem. 81, 8774–8782.
Lin, Z.A., et al., 2011. J. Mater. Chem. 21, 518–524.
Link, S., El-Sayed, M.A., 1999. J. Phys. Chem. B 103, 4212–4217.
Liu, S., et al., 2005. Chem. Eur. J. 11, 4239–4246.
Liu, Y., Feng, X., Shen, J., Zhu, J., Hou, W., 2008. J. Phys. Chem. B 112, 9237–9242.
Luo, X.L., Xu, J.J., Du, Y., Chen, H.Y., 2004. Anal. Biochem. 334, 284–289.
Ma, Y., Li, N., Yang, C., Yang, X., 2005. Colloids Surf. A 269, 1–6.
Mader, H.S., Wolfbeis, O.S., 2008. Microchim. Acta 162, 1–34.
Mateo, C., Palomo, J.M., Fernandez-Lorente, G., Guisan, J.M., Fernandez-Lafuente, R., 2007. Enzyme Microb. Technol. 40, 1451–1463.
Matsumoto, A., Sato, N., Kataoka, K., Miyahara, Y., 2009. J. Am. Chem. Soc. 131, 12022–12023.
Nien, P., Wang, J., Chen, P., Chen, L., Ho, K., 2010. Bioresour. Technol. 101, 5480–5486.
Pham, T.A., Kumar, N.A., Jeong, Y.T., 2010. Colloids Surf. A 370, 95–101.
Qiu, H., et al., 2009. Biosens. Bioelectron. 24, 3014–3018.
Rahman, M.A., Kwon, N.H., Won, M.S., Choe, E.S., Shim, Y.B., 2005. Anal. Chem. 77, 4854–4860.
Rakhi, R.B., Sethupathi, K., Ramaprabhu, S., 2009. J. Phys. Chem. B 113, 3190–3194.
Sanchez, C., Belleville, P., Popall, M., Nicole, L., 2011. Chem. Soc. Rev. 40, 696–753.
Sarma, A.K., Vatsyayan, P., Goswami, P., Minteer, S.D., 2009. Biosens. Bioelectron. 24, 2313–2322.
Seker, E., Reed, M.L., Begley, M.R., 2009. Materials 2, 2188–2215.
Shim, J., Kim, G.Y., Moon, S.H., 2011. J. Electroanal. Chem. 653, 14–20.
Shoji, E., Freund, M.S., 2001. J. Am. Chem. Soc. 123, 3383–3384.
Springsteen, G., Wang, B., 2002. Tetrahedron 58, 5291–5300.
Tan, Y., et al., 2009. Biosens. Bioelectron. 24, 2225–2231.
Tan, Y., et al., 2010. J. Phys. Chem. B 114, 5016–5024.
Tan, Y., et al., 2008. Electroanalysis 20, 1599–1606.
Tang, D., Yuan, R., Chai, Y., 2008. Anal. Chem. 80, 1582–1588.
Thibault, S., Aubriet, H., Arnoult, C., Ruch, D., 2008. Microchim. Acta 163, 211–217.
Tokareva, I., Minko, S., Fendler, J.H., Hutter, E., 2004. J. Am. Chem. Soc. 126, 15950–15951.
Trasatti, S., Petrii, O., 1991. Pure Appl. Chem. 63, 711–734.
Wang, J., 2008. Chem. Rev. 108, 814–825.
Wu, B., et al., 2007. Biosens. Bioelectron. 22, 838–844.
Xu, Y., et al., 2009. Anal. Chem. 81, 503–508.
Xue, M.H., Xu, Q., Zhou, M., Zhu, J.J., 2006. Electrochem. Commun. 8, 1468–1474.
Yan, Y., Yehezkeli, O., Willner, I., 2007. Chem. Eur. J. 13, 10168–10175.
Yang, W., Wang, J., Zhao, S., Sun, Y., Sun, C., 2006. Electrochem. Commun. 8, 665–672.
Yao, N., Yao, G., Deng, C., Zhang, X., Yang, P., 2008. Chem. Commun., 5577–5579.
Yeap, W.S., Tan, Y.Y., Loh, K.P., 2008. Anal. Chem. 80, 4659–4665.
Yu, C., Yen, M., Chen, L., 2010. Biosens. Bioelectron. 25, 2515–2521.
Zayats, M., Katz, E., Willner, I., 2002a. J. Am. Chem. Soc. 124, 14724–14735.
Zayats, M., Katz, E., Willner, I., 2002b. J. Am. Chem. Soc. 124, 2120–2121.
Zhang, J., Song, S., Wang, L., Pan, D., Fan, C., 2007. Nat. Protoc. 2, 2888–2895.
Zhang, S., Wang, N., Yu, H., Niu, Y., Sun, C., 2005. Bioelectrochemistry 67, 15–22.
Zhang, X., Wu, Y., Tu, Y., Liu, S., 2008. Analyst 133, 485–492.
Zhang, Z., et al., 2011. J. Electroanal. Chem. 650, 241–247.
Zhao, S., Zhang, K., Bai, Y., Yang, W., Sun, C., 2006. Bioelectrochemistry 69, 158–163.
Zhong, X., Bai, H., Xu, J., Chen, H., Zhu, Y., 2010. Adv. Funct. Mater. 20, 992–999.
Zhou, Q., et al., 2007. J. Phys. Chem. B 111, 11276–11284.
Zhou, Y., Itoh, H., Uemura, T., Naka, K., Chujo, Y., 2002. Langmuir 18, 277–283.